available at www.sciencedirect.com

SCIENCE DIRECT®

journal homepage: www.elsevier.com/locate/biochempharm

In vitro and *in vivo* studies of a novel potential anticancer agent of isochaihulactone on human lung cancer A549 cells

Yi-Lin Chen [a,b,1], Shinn-Zong Lin [a,b,1], Jang-Yang Chang [c,1], Yeung-Leung Cheng [f], Nu-Man Tsai [a,b,g], Shee-Ping Chen [a,b], Wen-Liang Chang [e,2], Horng-Jyh Harn [a,b,d,2,*]

[a] *Institute of Medical Sciences, Buddhist Tzu-Chi University, Hualien, Taiwan*
[b] *Department of Neuro-Medical Scientific Center, Buddhist Tzu Chi General Hospital, Hualien, Taiwan*
[c] *Division of Cancer Research, National Health Research Institute, Taipei, Taiwan*
[d] *Department of Pathology, Emergency medicine, Buddhist Tzu Chi General Hospital, Hualien, Taiwan*
[e] *School of Pharmacy, National Defense Medical Center, Taipei, Taiwan*
[f] *Division of Thoracic Surgery, Department of Surgery, Tri-Service General Hospital, National Defense Medical Center, Taipei, Taiwan*
[g] *Department of Applied Life Science, Asia University, Taichung, Taiwan*

ARTICLE INFO

Article history:
Received 14 February 2006
Accepted 21 April 2006

Keywords:
Bupleurum scorzonerifolium
Isochaihulactone
Microtubule destabilizing
Apoptosis
Cell cycle arrest

ABSTRACT

We previously demonstrated that the crude acetone extract of *Bupleurum scorzonerifolium* (BS-AE) 60 μg/ml has anti-proliferation activity and apoptotic effects on A549 non-small cell lung cancer (NSCLC). A novel lignan, isochaihulactone (4-benzo[1,3]dioxol-5-ylmethyl-3(3,4,5-trimethoxyl-benzylidene)-dihydro-furan-2-one), was isolated from BS-AE and identified from spectral evidence (^{1}H NMR, ^{13}C NMR, IR, and MS) and by comparison with authentic synthetic standards. Isochaihulactone was cytotoxic (IC_{50} = 10–50 μM) in a variety of human tumor cell lines. In *in vitro* and *in vivo* microtubule assembly assays, it inhibited tubulin polymerization in a concentration-dependent manner. As determined by flow cytometry, isochaihulactone caused G2/M phase arrest and apoptosis in a time- and concentration-dependent manner. G2/M arrest was correlated with increased p21/WAF1 levels, downregulation of the checkpoint proteins cyclin B1/cdc2 and mobility shift of cdc25C. Moreover, isochaihulactone (30 and 50 mg/kg) inhibited the growth of non-small cell lung carcinoma A549 xenograft in nude mice. These findings indicate isochaihulactone is a promising new antimitotic anticancer compound with potential for clinical application in the future.

1. Introduction

Cancers present a serious clinical problem and pose significant social and economic impacts on the health care system. Despite improved imaging and molecular diagnostic techniques, the disease still impacts millions of patients worldwide [1]. Interfering with tubulin's normal biological function is a clinically proven approach for treating various types of tumors. Compounds that bind to β-tubulin, such as taxanes and the *Vinca* alkaloids, interfere with tubulin polymerization and microtubule depolymerization and thereby disrupt normal cell division and commit the cell to apoptosis [2–4].

* *Corresponding author at*: Neuro-Medical Scientific Center, Department of Pathology, Tzu-Chi General Hospital, 707, Section 3, Chung-Yang Road, 970 Hualien, Taiwan. Tel.: +886 3 8561825x2223; fax: +886 3 8564656.
E-mail address: duke@tzuchi.com.tw (H.-J. Harn).

[1] The first three authors contributed equally to this work.
[2] The last two authors contributed equally to this work.

0006-2952/$ – see front matter © 2006 Elsevier Inc. All rights reserved.
doi:10.1016/j.bcp.2006.04.031

Although taxanes and *Vinca* alkaloids are effective for the management of different malignancies, resistance to drugs like paclitaxel and vincristine frequently develops in some tumors after an initial quick and promising response during chemotherapy [2,3]. This possibility increases the drastic social, economic, and psychological effects of cancer on patients; therefore, novel anticancer components that overcome drug resistance and have improved pharmacology profiles are needed.

Living organisms, including plants, microbes, and marines organisms, provide rich sources of chemically diverse bioactive compounds [5]. More than 40% of the chemicals, thus far identified as natural products, have not been chemically synthesized. Natural products and their derivatives including vinblastine, paclitaxel, and etoposide already play critical roles in cancer chemotherapy [5–10]. Chinese herbal medicine books (such as Shen Nung Pen Tsao Ching [220 AD] and the Pharmacopoeia of China) provide a wealth of information about plants and anticancer herbal formulations that are a useful starting point for the identification of new anticancer compounds [11–15].

Nan-Chai-Hu (Chai Hu of the South), the root of *Bupleurum scorzonerifolium*, is an important Chinese herb in the treatment of influenza, fever, malaria, cancer, and menstrual disorders in China, Japan, and many other parts of Asia. It is also a major ingredient of traditional Chinese medicine formulations such as Sho-Saiko-To-Tang (TJ9 in Japan) and Bu-Zhong-Yi-Qi-Tang. We have previously shown that the Chai Hu extracts contain potent ingredients against tumor growth and induce tumor apoptosis [16,17]. In addition, the acetone extract of Chai Hu (BS-AE) exhibits strong antagonistic activity toward telomerases in the human lung cancer derived cell line, A549 [16]. These results prompted us to examine the chemical composition profile of Chai Hu and identify the active anticancer components.

We previously reported that the crude acetone extract of *B. scorzonerifolium* (BS-AE) causes A549 cell cycle G2/M phase arrest, formation of giant cells, and apoptosis [16,17]. This manuscript describes the identification of a novel lignan, isochaihulactone, which causes microtubule depolymerization, cell cycle arrest, and pro-apoptotic activities in A549 cells. We provide evidence that the disruption of the regular cell cycle at G2/M phase and the activation of phospho-Bcl-2 and caspase-3 is important in isochaihulactone-induced apoptosis. Furthermore, we identified isochaihulactone as a potential antitumor drug based on its extreme cytotoxicity in A549 cells and *in vivo* antitumor activity against human A549 xenograft in nude mice.

2. Materials and methods

2.1. Fraction purification of isochaihulactone and structure determination

B. scorzonerifolium roots were supplied from Chung-Yuan Co., Taipei, and the plant was identified by Professor Lin of the National Defense Medicinal Center, where a voucher specimen was deposited (NDMCP No. 900801). The acetone extract AE-BS was prepared as described previously [15]. The AE-BS dissolved in 95% MeOH solution and then partitioned (1:1) with *n*-hexane to give the *n*-hexane-soluble fraction (BS-HE). The aqueous 95% MeOH layer was evaporated to remove residual MeOH, and then distilled water was added. This aqueous solution was further partitioned with $CHCl_3$ to get the $CHCl_3$-soluble fraction (BS-CE) and H_2O-soluble fraction (BS-WE). The BS-CE was subjected to chromatography over silica gel and eluted with CH_2Cl_2, CH_2Cl_2–MeOH (95:5), CH_2Cl_2–MeOH (9:1), CH_2Cl_2–MeOH (8:2) and MeOH, successively. The bioactive component, BS-CE-E02, was applied to silica gel and eluted with CH_2Cl_2–MeOH (99:1) to obtain isochaihulactone. The pure compound, isochaihulactone forms white needle crystals with a physical properties of mp 137–138 °C; $[\alpha]_D^{25}$ −29.0° (*ca.* 0.5, $CHCl_3$); IR (KBr) ν_{max} cm^{-1}: 1745, 1635, 1581, 1335, 1153; UV ($CHCl_3$) λ_{max} nm (log ε): 247 (4.08), 298 (4.17), 327 (4.08); ^1H NMR ($CDCl_3$) δ: 3.29 (1H, m, H-3), 4.10 (1H, dd, J = 9.0, 3.8 Hz, H-4α), 4.31 (1H, dd, J = 9.0, 7.3 Hz, H-4β), 6.60 (1H, d, J = 1.5 Hz, H-5), 2.78 (1H, dd, J = 13.7, 9.0 Hz, H-6α), 2.92 (1H, dd, J = 13.7, 6.7 Hz, H-6β), 7.24s (2H, s, H-2′, 6′), 6.67 (1H, d, J = 1.4 Hz, H-2″), 6.74 (1H, d, J = 7.8 Hz, H-5″), 6.61 (1H, dd, J = 7.8, 1.4 Hz, H-6″), 3.87 (9H, s, OMe), 5.93 (1H, d, J = 1.3 Hz, OCH_2O), 5.94 (1H, d, J = 1.3 Hz, OCH_2O); ^{13}C NMR ($CDCl_3$) δ: 169.29s (C-1), 126.36s (C-2), 44.43d (C-3), 69.82t (C-4), 140.60d (C-5), 40.72t (C-6), 128.83s (C-1′), 108.65d (C-2′), 152.62s (C-3′), 139.61s (C-4′), 152.62s (C-5′), 108.65d (C-6′), 131.31s (C-1″), 109.29d (C-2″), 147.94s (C-3″), 146.49s (C-4″), 108.39d (C-5″), 122.29d (C-6″), 56.18q (2′-OMe), 60.90q (3′-OMe), 56.18q (4′-OMe), 101.03t (OCH_2O); EIMS, 70 eV, m/z (rel. int.): 398 ([M]$^+$, 18), 263 (100), 207 (16), 135 (35).

2.2. Chemicals and reagents

Isochaihulactone was dissolved in DMSO to a concentration of 50 mM and stored in −20 °C as a master stock solution. Dimethyl sulfoxide (DMSO), 3-(4,5-dimethyl thizol-2-yl)-2,5-diphenyl tetrazolium bromide (MTT), propidium iodine (PI), RNase A, Hoechst 33342, paclitaxel, vincristine colchicines, p53, p21, α-tubulin, horseradish peroxidase-conjugated and FITC-conjugated secondary antibodies were purchased from Sigma Chemical Co. (St. Louis, MO, USA). Bcl-2 monoclonal antibody was purchased from Santa Cruz Biotechnology (Santa Cruz, CA). RPMI 1640 medium, Eagle's minimum essential medium, fetal bovine serum (FBS), penicillin, streptomycin, trypsin/EDTA, NuPAGE Bis–Tris Electrophoresis System (pre-cast polyacrylamide mini-gel) were purchased from Invitrogen (Carlsbad, CA, USA). Mycoplasma Removal Reagent was from Dainippon Pharmaceutical Co. (Osaka, Japan). Annexin V-FLOUS Staining Kit was from Roche Molecular Biochemicals (Mannheim, Germany). Cyclin B1, cdc25C, cdc2, phosphor-Asp^{330} caspase-9, phosphor-Asp^{384} caspase-8, phosphor-Ser^{70} Bcl-2, caspase-3, PARP, β-actin antibodies were purchased from Cell signaling Technology. Polyvinyldenefluoride (PVDF) membranes, BSA protein assay kit and Western blot chemiluminescence reagent were purchased from Amersham Biosciences (Arlington Heights, IL).

2.3. Cell lines and culture

The A549 human lung adenocarcinoma cells, H520 human lung squamus cell carcinoma cells, H1299, the p53-null and p16-deficient human non-small cell human large cell carcinoma cells, HT29 human colon adenocarcinoma cells, MCF-7

human breast cancer cells, OVCAR-3 human ovarian cancer cells and DBTRG human brain cancer cells were obtained from American Type Culture Collection (Manassas, VA). The paclitaxel-resistant subline, A549-T12, with mutant Kα-1 tubulin, was kindly provided by Dr. Horwitz [18]. The KB Human cervical carcinoma cells and P-glycoprotein (P-gp) overexpression subline, KB-TAX50 were kindly provided by Chang [19]. The HepG2 human hepatoma cell lines was kindly provided by Chou and Yang [20]. A549, H520, H1299, HT 29, OVCAR-3, KB and DBTRG cancer cells were maintained with RPMI 1640 medium containing 10% FBS and 100 ng/ml each of penicillin and streptomycin at 37 °C in a humidified atmosphere with 5% CO_2. The A549-T12 and KB-TAX50 cells were maintained with 6 and 50 nM paclitaxel, respectively. MCF-7 and HepG2 cancer cells were maintained in Eagle's minimum essential medium with 10% FBS and 100 ng/ml each of penicillin and streptomycin at 37 °C in a humidified atmosphere with 5% CO_2. All cultures were free of mycoplasma.

2.4. Growth inhibition assay

Before the experiment, A549-T12 and KB-TAX50 cells were maintained for 1 week in 6 and 50 nM paclitaxel, respectively. The viability of the cells after treated with various chemicals was evaluated using MTT assay preformed in triplicate [21]. Briefly, the cancer cells (5×10^3) were incubated in 96-well plates containing 200 μl of the culture medium. Cells were permitted to adhere for 12–18 h then washed with phosphate buffered saline (PBS). Solutions were always prepared fresh by dissolving 0.2% DMSO or drugs in culture medium and added to various kind of tumor. After 48 h of exposure, the drug-containing medium was removed, washed with PBS and replaced by fresh medium. The cells in each well were then incubated in culture medium with 500 μg/ml MTT for 4 h. After the medium were removed, 200 μl of DMSO and 25 μl of glycine buffer (0.1 M glycine, 0.1 M NaCl, pH 10.5) were added to each well. Absorbance at 570 nm of the maximum was detected by a PowerWave X Microplate ELISA Reader (Bio-TeK Instruments, Winoski, VT). The absorbance for DMSO treated cells was considered as 100%. The results were determined by three independent experiments.

2.5. In vitro microtubule assembly assay

The assay was basically performed according to Bollag et al. [22]. In brief, microtubule-associated protein-rich tubulin in 100 μl buffer containing 100 mM PIPES (pH 6.9), 2 mM MgCl2, 1 mM GTP, and 2% (v/v) DMSO was placed in 96-well microtiter plates in the presence of test agents. The increase in absorbance was measured at 350 nm in a PowerWave X Microplate Reader at 37 °C and recorded every 30 s for 30 min. The area under the curve was used to determine the concentration that inhibited tubulin polymerization by 50% (IC_{50}). The area under the curve of the untreated control was set 100% polymerization, and the IC_{50} was calculated by nonlinear regression.

2.6. In vivo microtubule assembly assay

A method described by Blagosklonny et al. was used to quantify the amount of free versus polymerized tubulin [23]. Approximately 2×10^6 cells were cultured in six-well plates and treated the following day with chemicals and various herbal extracts. After 24 h of exposure, cells were washed twice with PBS and lysed in 100 μl of hypotonic buffer (20 mM Tris–HCl, pH 6.8, 1 mM $MgCl_2$, 2 mM EGTA, 1% Nonidet P-40, 2 mM phenylmethylsulfonyl fluoride, 1 μm/ml aprotinin and 2 μg/ml pepstatin) at 37 °C for 5 min.

The cell lysate in which the cytosolic and cytoskeleton fractions containing soluble and insoluble tubulin, respectively, was separated by centrifugation. The cytoskeletal pellet was resuspended in 100 μl of hypotonic buffer with 20 μl of sample loading buffer (45% glycerol, 20% β-mercaptoethanol, 9.2% SDS, 0.04% bromphenol blue, and 0.3 M Tris–HCl, pH 6.8) and boiled for 5 min. Electrophoresis was performed on NuPAGE Bis–Tris Electrophoresis System (10% NuPAGE Bis–Tris gels) using 20 μl of each sample. Immunoblotting was performed using monoclonal mouse anti-α-tubulin antibody conjugated to antimouse IgG–HRP antibody and detected by Western Lightning™ Chemiluminescence Reagent Plus and quantified using a densitometers.

2.7. Immunocytochemistry assay

Cells cultured on glass slides were treated with various concentrations of paclitaxel, colchicines and isochaihulactone for 12 h prior to fixation with cold 3.7% formaldehyde. The fixed cells were washed twice in PBS, and incubated in cold permeabilization solution (0.1% Triton X-100 + 0.1% sodium citrate). After inactivating endogenous peroxidase with 3% H_2O_2 the cells were washed with PBS again and incubated with an anti-α-tubulin antibody at room temperature. After 2 h of incubation, the cells were washed with PBS to remove excess antibody and then probed with FITC-conjugated secondary antibody 1 h at room temperature. The images of α-tubulin with FITC staining were taken with the Axiovert 200M fluorescence microscope (Carl Zeiss, Oberkochen, Germany).

2.8. Cell cycle analysis

The cell cycle was determined by flow cytometry with DNA staining to reveal the total amount of DNA. Approximately 5×10^5 of cells were incubated in various concentration of isochaihulactone for the indicated time. Cells were harvested by treating the cells with trypsin/EDTA. The cells were collected, washed with PBS, fixed with cold 70% ethanol overnight, and then stained with a solution containing 45 μg/ml PI, 10 μg/ml RNase A, and 0.1% Triton X-100 for 1 h in the dark. The cells will then pass through FACScan flow cytometer (equipped with a 488-nm argon laser) to measure the DNA content. The data was obtained and analyzed with CellQuest 3.0.1 (Becton Dickinson, Franklin Lakes, NJ) and ModFitLT V2.0 software.

2.9. Detection of apoptosis

The apoptosis was analyzed according to the method described by van Engeland et al. to detect the integrity of cellular membrane and the externalization of phosphatidylserine [24]. In brief, approximately 10^6 cells were grown in 35 mm diameter plates. The cells were incubated in various concentration of isochaihulactone for the indicated time and

then labeled with 10 μg/ml of Annexin V-FLOUS and 20 μg/ml of PI prior to harvesting. After labeling, the cells were washed with binding buffer and harvesting by scraping. Cells were resuspended in binding buffer at a concentration of 2×10^5 cells/ml before analysis by flow cytometry (FACScan). The data was analyzed on WinMDI V2.8 software. The percentage of cells undergoing apoptosis was determined by three independent experiments.

2.10. Western blot analysis

Approximately 5×10^6 cells were cultured in 100-mm^2 dishes and then incubated in various concentration of isochaihulactone for the indicated time. The cells were lysed on ice with 200 μl of lysis buffer (50 mM Tris–HCl, pH 7.5, 0.5 M NaCl, 5 mM $MgCl_2$, 0.5% nonidet P-40, 1 mM phenylmethylsulfonyl fluoridefor, 1 μg/ml pepstatin, and 50 μg/ml leupeptin) and centrifuged at 13,000 × *g* at 4 °C for 20 min. The protein concentrations in the supernatants were quantified using a BSA Protein Assay Kit Electrophoresis was performed on a NuPAGE Bis–Tris Electrophoresis System using 50 μg of reduced protein extract per lane. Resolved proteins were then transferred to polyvinyldenefluoride (PVDF) membranes. Filters were blocked with 5% non-fat milk overnight and probed with appropriate dilution of primary antibodies for 1 h at room temperature. Membranes were washed with three times with 0.1% Tween 20 and incubated with HRP-conjugated secondary antibody for 1 h at room temperature. All proteins were detected using Western Lightning™ Chemiluminescence Reagent Plus and quantified using a densitometers.

2.11. Antitumor activity in vivo

Xenograft mice as a model system to study cytotoxicity effect of isochaihulactone *in vivo*: the implantation of cancer cells were carried out similarly to previous reports. Female congenital athymic BALB/c nude (nu/nu) mice were purchased from National Sciences Council (Taipei, Taiwan) and all procedures were performed in compliance with the standard operating procedures of the Laboratory Animal Center of Tzu Chi University (Hualien, Taiwan). All experiments were carried out using 6–8-week old mice weighing 18–22 g. The animals were s.c. implanted with 1×10^7 cells into the back of mice. When the tumor reached 80–120 mm^3 in volume, animals were divided randomly into control and test groups consisting of six mice per group (day 0). Daily s.c. administration of isochaihulactone, dissolved in a vehicle of 20% Tween 80 in normal saline (v/v) was performed from days 0 to 4 far from the inoculated tumor sites (>1.5 cm). The control group was treated with vehicle only. The mice were weighed three times a week up to days 21–28 to monitor the effects and the same time the tumor volume was determined by measurement of the length (*L*) and width (*W*) of the tumor. The tumor volume at day *n* (TV_n) was calculated as TV (mm^3) = ($L \times W^2$)/2. The relative tumor volume at day *n* (RTV_n) versus day 0 was expressed according to the following formula: $RTV_n = TV_n/TV_0$. Tumor regression (T/C (%)) in treated versus control mice was calculated using: T/C (%) = (mean RTV of treated group)/(mean RTV of control group) × 100. Xenograft tumors as well as other vital organs of treated and control mice were harvested and fixed in 4% formalin, embedded in paraffin, and cut in 4-μm sections for histologic study.

2.12. Statistical analysis

The data was shown as mean with standard deviation. The statistical difference was analyzed using the Student's *t*-test for normal distributed values and by nonparametric Mann–Whitney *U* test for values of non-normal distribution. Values of $P < 0.05$ were considered significant.

3. Results

3.1. Isochaihulactone inhibited cell proliferation and induced morphology change in human cancer cells

In our previous study, we demonstrated that the BS-AE inhibited A549 cell proliferation more effectively than did BS-WE [15]. These cell proliferation assay results clearly indicate that the bioactive component is preserved in the BS-AE. Silica gel column elution with different solvent systems and TLC were used to elucidate the chemical composition of BS-AE. MTT assay revealed that isochaihulactone (a novel lignan with the chemical formula $C_{22}H_{22}O_7$ based on spectral analyses) had a strong anti-proliferative effect on A549 cells. The isochaihulactone contains two C_6–C_3 units, a structural signature of lignan family compounds (Fig. 1). Compared to the untreated cells, isochaihulactone-treated A549 cells showed obvious cell shrinkage and chromosomal fragmentation typical of cells undergoing apoptosis. Isochaihulactone caused cytotoxicity in various cancer cell lines including lung, breast, ovary, colon, liver tumor cells (IC_{50} = 10–50 μM after 48 h), paclitaxel-resistant A549-T12 and P-gp-overexpression KB-TAX50 cells (Table 1).

Fig. 2B and C shows the changes in A549 cell morphology after treatment with isochaihulactone for 1 and 2 days. Morphology was obviously after treatment with isochaihulactone for 2 days. Compared to untreated cells (Fig. 2A), numerous isochaihulactone-treated cells were flatter, enlarged, and had vacuolated cytoplasm (Fig. 2C). After 24 h treatment of isochaihulactone, most cells showed nuclear disorganization with perturbed and condensed chromatin (Fig. 2D).

3.2. Isochaihulactone destabilized microtubule polymerization

Isochaihulactone has been suggested to act like certain cytotoxic chemicals (such as paclitaxel and vinblastine) that

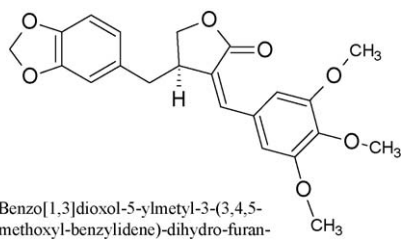

4-Benzo[1,3]dioxol-5-ylmetyl-3-(3,4,5-trimethoxyl-benzylidene)-dihydro-furan-2-one

MW=398.41

Fig. 1 – Chemical structure of isochaihulactone.

Table 1 – Growth inhibition of various compounds against human tumor cell lines

Cell lines	Origin	Growth inhibition (IC_{50})[a]		
		Isochaihulactone (μM)[b]	Vincristine (nM)	Paclitaxel (nM)
A549	Lung adenocarcinoma	18.5 ± 5.1	2.2 ± 0.3	2.6 ± 0.5
A549-T12	Lung adenocarcinoma	9.4 ± 2.2	2.4 ± 0.5	18.1 ± 0.2
H520	Lung squamus carcinoma	17.1 ± 5.0	2.7 ± 0.2	5.2 ± 1.3
H1299	Lung adenocarcinoma	25.4 ± 7.1	1.8 ± 0.4	4.5 ± 1.0
HT-29	Coloretal adenocarcinoma	30.4 ± 9.9	1.1 ± 0.5	8.2 ± 0.3
MCF-7	Breast adenocarcinoma	39.6 ± 11.6	1.2 ± 0.3	2.1 ± 0.4
HepG2	Hepatocellular adenocarcinoma	12 .1 ± 5.4	6.0 ± 1.2	6.5 ± 1.7
OVCAR-3	Ovarian adenocarcinoma	17.2 ± 9.2	1.4 ± 0.3	2.3 ± 0.6
DBTRG	Brain glioblastoma	49.7 ± 12.1	2.1 ± 1.0	10.0 ± 0.4
KB	Oral epidermoid carcinoma	23.2 ± 4.2	0.5 ± 0.1	5.4 ± 0.8
KB-TAX50	Oral epidermoid carcinoma	26.3 ± 3.5	2.3 ± 0.4	250.6 ± 12.1

[a] IC_{50}, drug concentration that inhibits cell division by 50% after 48 h (mean ± S.D. from three independent experiments).
[b] Isochaihulactone, 4-benzo[l,3]dioxol-5-ylmetyl-3-(3,4,5-trimethoxyl-benzylidene)-dihydro-furan-2-one.

disrupt polymerized tubulin and the balance between depolymerized and polymerized tubulin in cells. To test this hypothesis, the effect of isochaihulactone on tubulin polymerization was first examined *in vitro*. Fig. 3A shows the result of microtubule assembly *in vitro* using microtubule-associated protein (MAP)-rich tubulin. In control samples, absorbance at 350 nm (A_{350}) increased with time. In the presence of 5 μM colchicines, tubulin polymerization was inhibited more than 75% compared with that of the control sample. Furthermore, in the presence of isochaihulactone, tubulin polymerization was inhibited in a concentration-dependent manner. The inhibitory concentration that

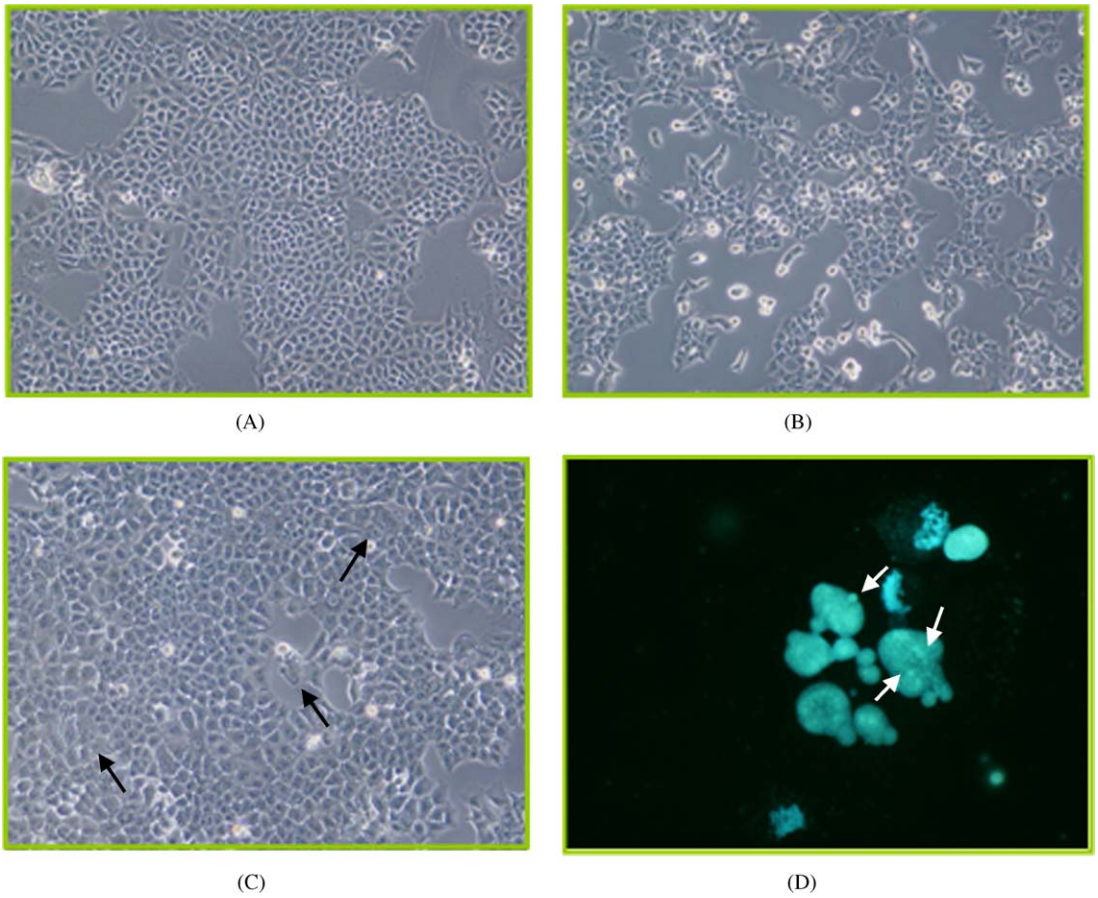

Fig. 2 – Effects of morphology and chromatin change of isochaihulactone in A549 cells. Morphological examination of isochaihulactone-induced giant cells. Cells were treated with 20 μM isochaihulactone for 1 and 2 days (B and C) compared to control, 0.2% DMSO (A). Cells were visualized by microscopy (A–C, magnification 200×). Detection of chromatin change with the Hoechst 33342 cell staining. Cells were treated with 20 μM isochaihulactone for 24 h (D) and cells were visualized by fluorescence microscopy (magnification 400×). Isochaihulactone-treated cells with condensed chromatin and indicated by arrow.

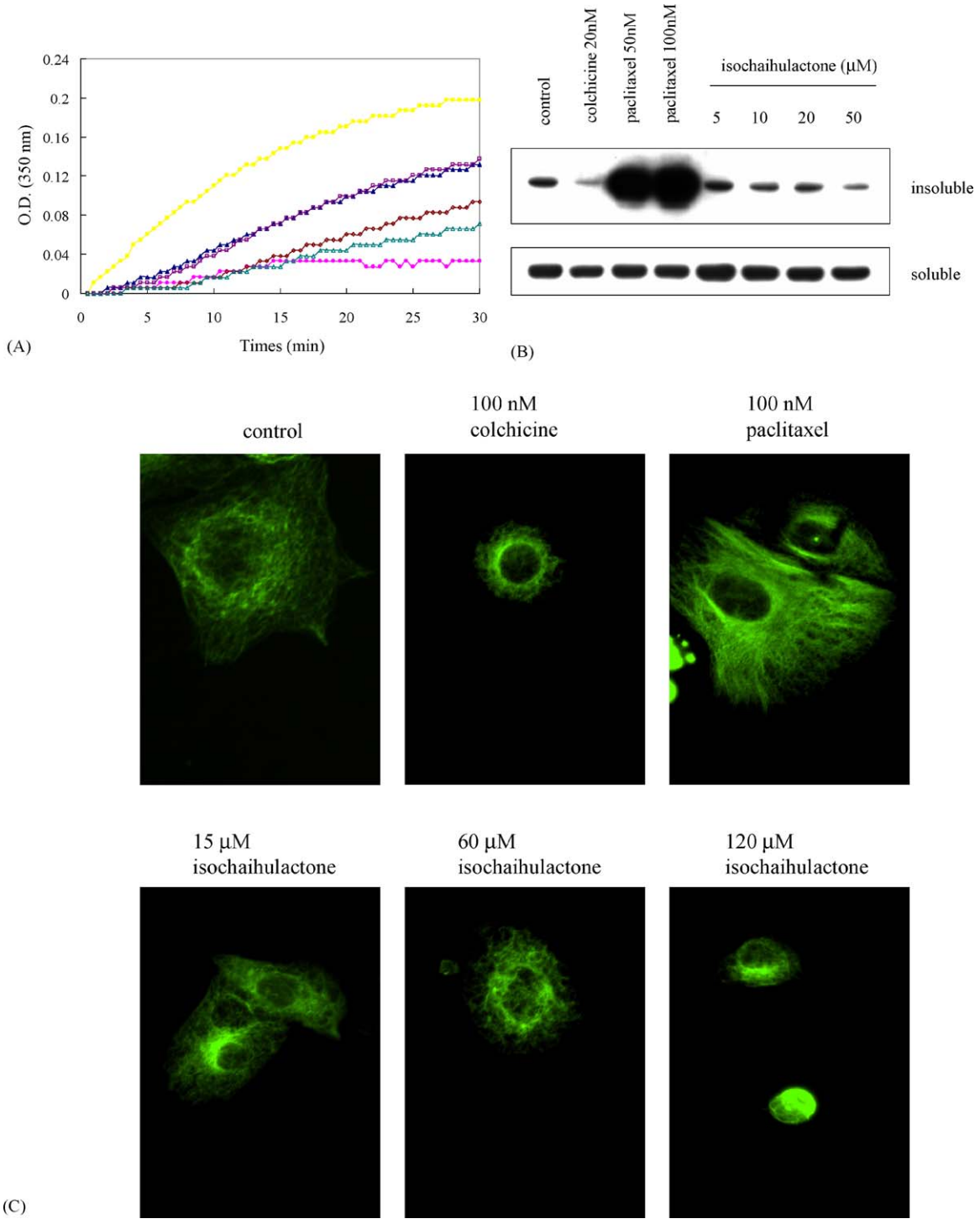

Fig. 3 – Effects of isochaihulactone on tubulin assembly *in vitro*. and *in vivo*. (A) Isochaihulactone-induced tubulin depolymerization *in vitro*. MAP-rich tubulin protein in a reaction buffer was incubated at 37 °C in the absence of drug (control, ▲) or presence of colchicines (5 μM, ●), paclitaxel (10 nM, ■), isochaihulactone (10 μM, □; 25 μM, ◇; 50 μM, △). Colchicines (5 μM, ●) was used as a microtubule depolymerization positive control and paclitaxel (10 nM, ■) was used as a microtubule polymerization positive control. (B) Isochaihulactone inhibited tubulin polymerization *in vivo*. A549 cells were treated with colchicines (20 nM), paclitaxel 50 and 100 nM, and 5, 10, 20 and 50 μM isochaihulactone for 24 h. Cell lysates were centrifuged to separate polymerized microtubules from tubulin dimmers as described in Section 2. After gel electrophoresis and transfer to nitrocellulose membrane, α-tubulin was visualized by Western blot analysis. (C) Isochaihulactone caused cellular microtubule abnormal organization and arrangement in A549 cells. A549 cells were treated with 0.2% DMSO (control), 100 nM clochicline, 100 nM paclitaxel and isochaihulactone ranging from 15 to 120 μM for 12 h. Fixed cells were reacted with anti-α-antibody for 2 h and then reacted with FITC-conjugated secondary antibody. The cells were visualized by Zeiss Axiovert 200M fluorescence microscopy. The images were representative of two independent experiments.

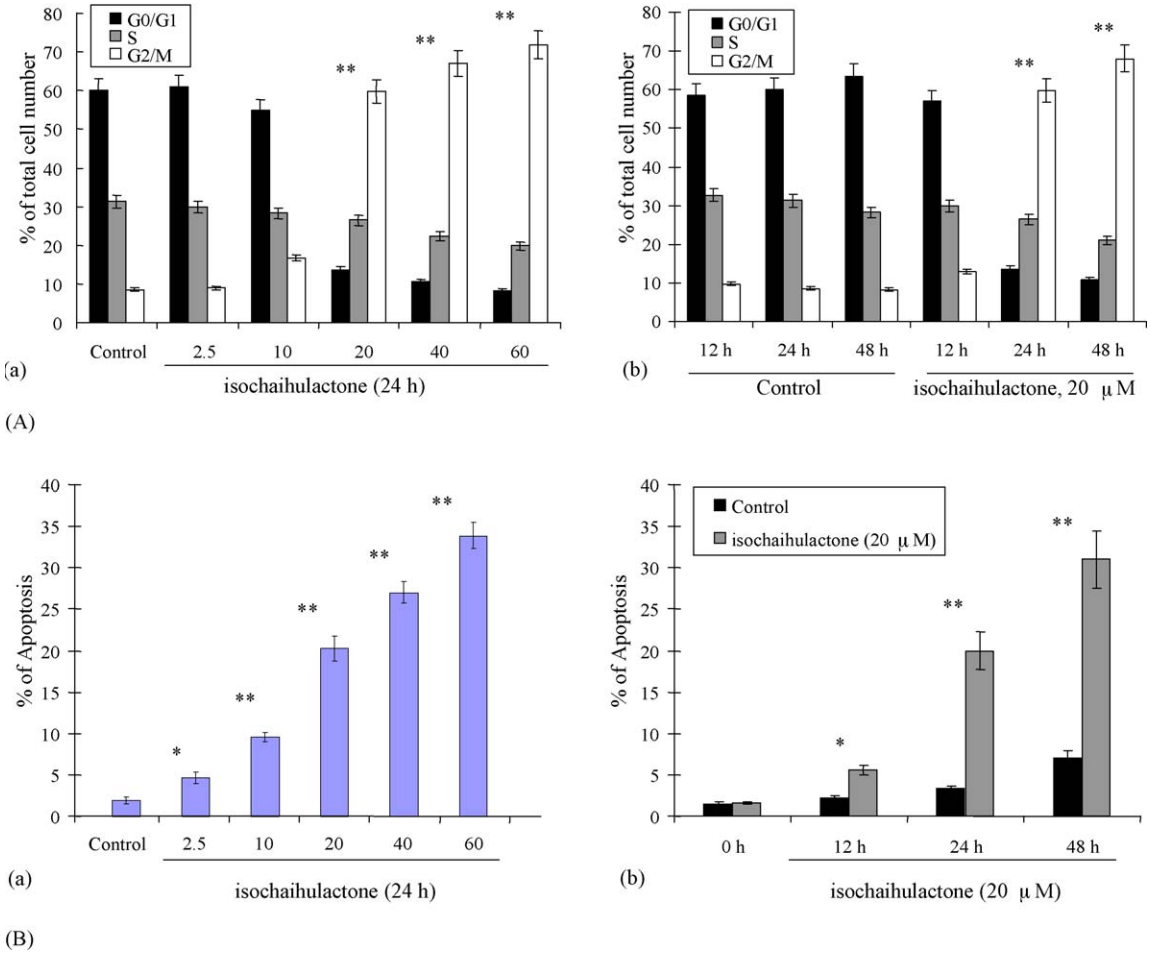

Fig. 4 – Effect of isochaihulactone-induced G2/M phase arrest and apoptosis in A549 cells. (A) Isochaihulactone-induced cell cycle G2/M arrest in A549 cells. Cells were treated with different concentration ranging from 2.5 to 60 μM for 24 h (a) and cells were treated 20 μM isochaihulactone with duration time ranging from 12 to 48 h (b). The cell cycle analysis was done as described in Section 2. (B) Isochaihulactone-induced apoptosis in A549 cells. Cells were treated with different concentration ranging from 2.5 to 60 μM for 24 h (a) and cells were treated 20 μM isochaihulactone with duration time ranging from 12 to 48 h (b). Apoptosis was detected by Annexin V-FLOUS Staining Kit and as described in Section 2. Data represent means ± S.D. from three independent experiments performed in duplicate. $^{*}P < 0.05$; $^{**}P < 0.01$ vs. the control.

inhibited tubulin polymerization by 50% (IC_{50}) was 25 ± 5 μM ($n = 3$). An *in vivo* microtubule assembly assay (Fig. 3B) showed that both isochaihulactone and colchicines significantly, concentration-dependently inhibited tubulin polymerization whereas paclitaxel promoted tubulin polymerization. As shown in Fig. 3C, the use of immunofluorescence techniques revealed that the organization and arrangement of microtubules in control cells was normal. Treatment with colchicines (100 nM) or isochaihulactone (15–120 μM, 12 h) in a dose-dependent manner caused observable microtubule disassembly, whereas 100 nM paclitaxel caused tubulin polymerization (Fig. 3C).

3.3. *Isochaihulactone-induced cell cycle arrest in G2/M phase and induced apoptosis in A549 cells*

To elucidate isochaihulactone's mode of action, isochaihulactone's effect on cell cycle progression was examined. Flow cytometry analysis showed that isochaihulactone treatment resulted in the accumulation of cells in G_2/M phase in a time- and dose-dependent manner (Fig. 4A). It was suggested that isochaihulactone may, like paclitaxel or vinblastine, caused G_2/M phase arrest. Simultaneous staining with Annexin V-FLOUS and PI revealed that about 30–50% of the isochaihulactone-treated cells were in early apoptotic stages. Furthermore, isochaihulactone-induced apoptosis in a time- and concentration-dependent manner (Fig. 4B).

3.4. *Isochaihulactone changed phosphorylation status of G2/M regulators and induced apoptosis*

To determine the relationship between isochaihulactone-induced mitotic arrest, p53, p21, cdc25C, cyclin B1/cdc2 activities and Bcl-2 phosphorylation, we initially examined the status of these G2/M regulatory proteins in A549 cells treated with 20 μM isochaihulactone for 24 h. As shown in Fig. 5A, slower migrating forms of phosphatase cdc25C was present, indicative of changes in the phosphorylation state of

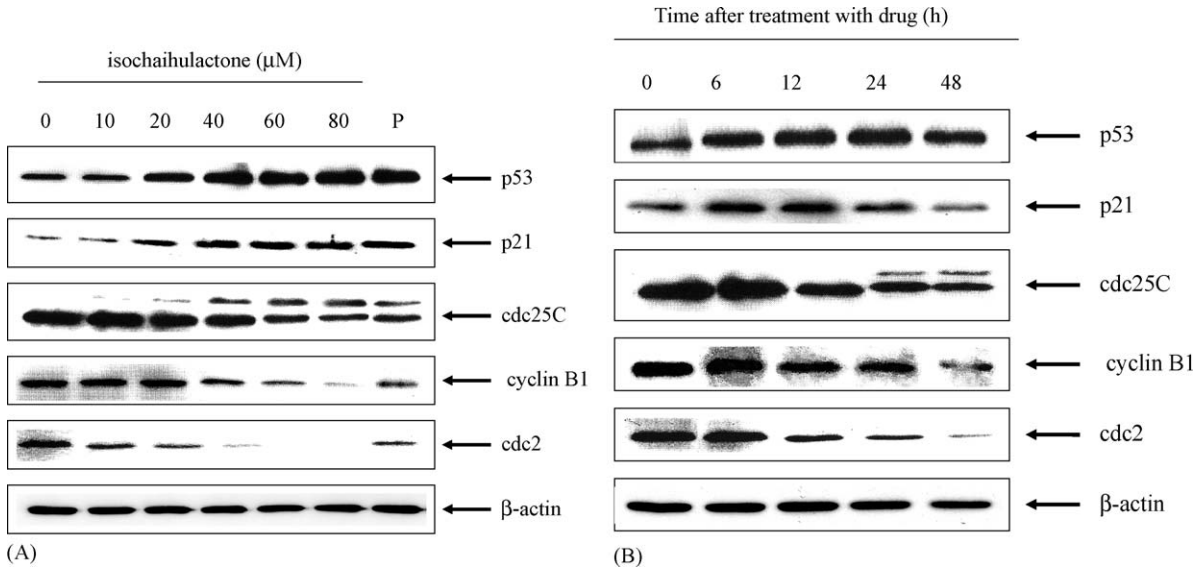

Fig. 5 – Isochaihulactone-induced changes in the phosphorylation status of G2/M regulatory proteins. Cells were treated with different concentration ranging from 10 to 80 μM for 24 h (A) and cells were treated 20 μM isochaihulactone with duration time ranging from 6 to 48 h (B). Five nanomolar pacliatxel (P) was used as a positive control. The Western blot analysis was done and as described in Section 2. Cells were probed with p53, p21, cyclin B1, cdc25C, cdc2 antibodies. Expression of β-actin was used as an internal control.

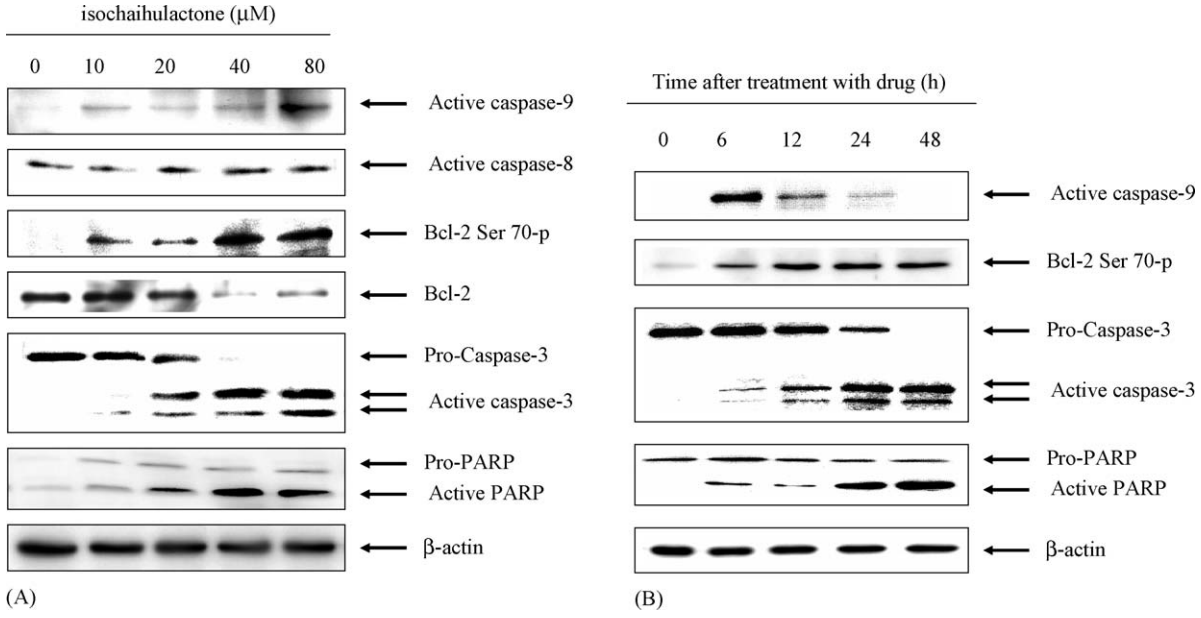

Fig. 6 – Isochaihulactone initiates Bcl-2 phosphorylation and caspase activation in A549 cells. (A) Isochaihulactone-induced caspase-3 activation and cleavage of PARP. Cells were treated with isochaihulactone for various concentrations for 24 h. The Western blot analysis was done and as described in Section 2. Cells were probed with phosphor-Asp^{330} caspase-9, phosphor-Asp^{384} caspase-8, phosphor-Ser^{70} Bcl-2, Bcl-2, caspase-3 and PARP antibodies. Expression of β-actin was used as an internal control. (B) Isochaihulactone-induced caspase-9 activation, followed by Bcl-2 phosphorylation and then caspase-3 activation. Cells were treated with 20 μM isochaihulactone for the indicated time and analysis by Western blot analysis. Cells were probed with phosphor-Asp^{330} caspase-9, phosphor-Ser^{70} Bcl-2, caspase-3, PARP antibodies. Expression of β-actin was used as an internal control.

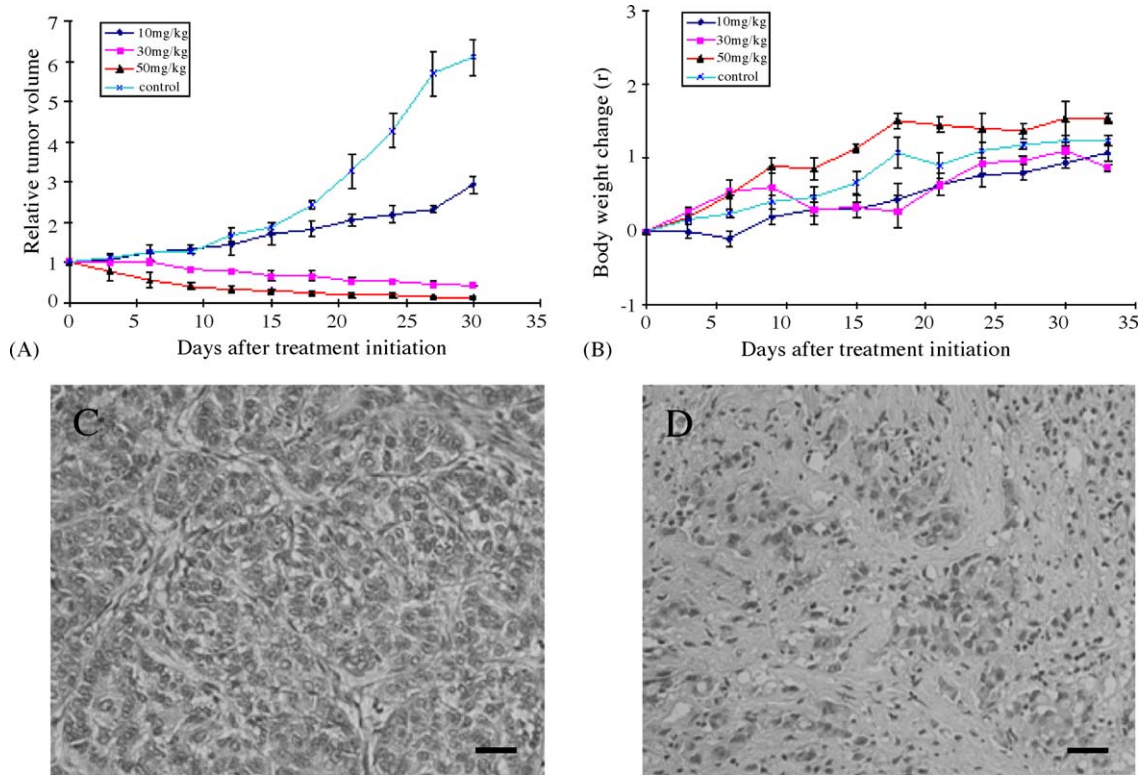

Fig. 7 – Inhibition of human xenografts growth *in vivo* by isochaihulactone. A549 tumor-bearing mice were administered s.c. with vehicle control (□), 10 mg/kg (◆), 30 mg/kg (■) or 50 mg/kg (▲) isochaihulactone on days 0–4 for 5 days. The figures shows the relative tumor volume (A) and body weight (B) of control and therapeutic groups. (C) shows the control A549 xenograft tumor and (D) shows the A549 xenograft tumor after administration of 50 mg/kg isochaihulactone at day 12; Scale bars, 100 μm. Data represent means ± S.D. of tumor volume and body weight at each time point.

these proteins. With increase in isochaihulactone concentration from 10 to 80 μM, upregulation of p53 and p21 and downregulation of cyclin B1/cdc2 kinases were also observed. Isochaihulactone-induced p53, p21 activation and downregulation of cyclin B1/cdc2 kinases were also in a time-dependent manner (Fig. 5B). Since activation of the caspases and cleavage of PARP is a crucial mechanism for induction of apoptosis and initiator caspases (*e.g.*, caspase-1, -2, -8, -9, and -10) are involved in the early stages of the proteolytic cascade, their involvement in isochaihulactone-induced apoptosis was investigated in A549 cells. Besides, the Bcl-2 protein located on the outer mitochondrial membrane is important for suppression of mitochondrial manifestations of apoptosis [25]. We examined whether isochaihulactone-induced apoptosis is associated with Bcl-2 phosphorylation. As shown in Fig. 6A, caspase-9 and caspase-3 was activated in a dose-dependent manner after isochaihulactone treatment. Thus, isochaihulactone-induced apoptosis is mediated through a caspase-dependent pathway. We also observed that caspase-9 activation, Bcl-2 phosphorylation, cleavage of caspase-3 and PARP in a time-dependent manner (Fig. 6B).

3.5. *Isochaihulactone had in vivo anticancer activity*

To evaluate the antitumor activity of isochaihulactone *in vivo*, human lung cancer xenografts were established by s.c. injection of approximately 1×10^7 A549 cells on the backs of nude mice. After the tumor reached about 100 mm^3 in size, mice were randomized into vehicle control and treatment groups (six animals each) and given a daily s.c. injection of either 0 (control group), or 10, 30, and 50 mg/kg of isochaihulactone (treatment groups) for five successive days. It was showed that isochaihulactone inhibits growth of tumor at low doses and results to tumor regression at higher doses (Fig. 7A). Histological examination showed prominent growth inhibition (50 mg/kg, D12; Fig. 7C and D) and no observable histological changes in various normal tissues including brain, liver and kidney (data not shown). The body weight of the tumor-bearing mice treated with 50 mg/kg was slightly increased (Fig. 7B).

4. Discussion

Although *B. scorzonerifolium* has been widely used as an herbal medicine in China and Japan to treat a number of diseases (mainly liver disease), no pure compounds have been isolated from *B. scorzonerifolium* to prove its anticancer activity. Because the anti-proliferative effect of acetone extract of *B. scorzonerifolium* (BS-AE) on A549 cells via inducing apoptosis has been demonstrated in our preliminary study and the *in vivo* antitumor effect of BS-AE was also demonstrated [16,17], bioassay directed fractionation was performed to identify the bioactive components of BS-AE. Thirteen pure compounds, including 2 new lignans (isochaihulactone and chaihu-

naphthone) and 11 known compounds (nemerosin, isoscutellarein-8-methyl ether, oroxylin, wogonin, eugenin, saikochromone A, kaerophyllin, isokaerophyllin, (−)-yatein, chinensinaphthol, and 1,2,3,7-tetramethoxyxanthone) were isolated from BS-AE. Our study evaluated the cytoxicity of these compounds (data not shown) and found that only isochaihulactone had an anticancer effect on both A549 and paclitaxel-resistant A549-T12 cells. This is the first report to show that a pure compound from *B. scorzonerifolium* has an anticancer effect and the first study to investigate the molecular mechanism of its antitumor activity.

Our data demonstrate that isochaihulactone was efficacious against various models of human solid tumors (Table 1). Malignant tumors can be resistant to treatment with microtubule inhibitors taxanes and *Vinca* alkaloids [26] and the mechanism of this resistance is mediated by the overexpression of the 170-kDa P-glycoprotein drug efflux pump, which is encoded by the multidrug resistance-1 gene [27]. Isochaihulactone *in vitro* is also effective against the drug-resistant KB cell line, which overexpresses P-gp (Table 1). Resistance also mediated by the expression of tubulin isotypes and mutations that show impaired paclitaxel-driven tubulin polymerization. A549-T12 is a paclitaxel resistant/dependent A549 cell line with a α-tubulin mutation [18]. No obvious difference in inhibition by isochaihulactone (IC50) was seen between A549 and A549-T12 (Table 1). The A549-T12 cell line exhibited no cross-resistance to isochaihulactone. These results showed that isochaihulactone might be useful for treating drug-refractory tumors.

In this study, isochaihulactone induced depolymerization of tubulin and inhibited normal spindle formation in NSCLC cells, resulting in mitotic arrest and cell death (Fig. 2). Isochaihulactone inhibited tubulin polymerization and the pattern of tubulin polymerization inhibition was similar to that of colchicines and vincristine (Fig. 3A and B). Moreover, the immunocytochemical staining of tubulin showed isochaihulactone caused microtubule depolymerization (Fig. 3C). These results further confirmed that isochaihulactone should be categorized as a ''microtubule-depolymerizing agent.'' Antitubulin compounds are classified on the basis of their β-tubulin binding site. Most drugs that destabilize microtubules (MTs) appear to bind at one of two binding sites, including the colchicine and vinblastine sites [28,29]. The colchicines binding site appears to be in the middle of the tubulin dimer, and some colchicine analogues are designed to compete for this site [30,31]. Examination of the competitive effect of isochaihulactone on [^{3}H] colchicines binding to β-tubulin revealed that colchicine binding is reduced at high isochaihulactone concentration (data not shown). Thus, isochaihulactone may not share the colchicines binding site and its interaction with tubulin may be through other ways.

The tumor suppressor protein p53 plays a role in the molecular response to DNA damage. Acting as a DNA-binding transcription factor, it regulates specific target genes to arrest the cell cycle and initiate apoptosis. Following DNA damage, cyclin-dependent kinase inhibitor p21 is expressed in a p53-dependent or p53-independent manner [32]. p21 may help to maintain G2 cell cycle arrest by inactivating the cyclin B1/cdc2 complex, disrupting the interaction between proliferating cell nuclear antigen and cdc25C [33]. In the present study, increased levels of p53 and p21 proteins were expressed in response to treatment with isochaihulactone (Fig. 5). Because H1299 cells are p53 negative and also growth inhibited, we suggested that isochaihulactone-induced growth inhibition maybe through both p53-dependent and p53-independent pathway. It is well known that the transition from G2 phase to mitosis is triggered by the cdc25-mediated activation of the cyclin B1/cdc2 complex and cyclin B1/cdc2 activation is triggered when cdc25, a phosphatase, dephosphorylates Thr15 [34,35]. In our study, we found that isochaihulactone mediated A549 cell arrest at G2/M phase (Fig. 4A), the arrest being accompanied by decreases expression of cyclin B1 and cdc2 kinase. The decrease in the levels of cdc2 may be due to the decrease in cdc25 activation by phosphorylation, leading to subsequent G2 arrest (Fig. 5). Our results indicate that the isochaihulactone-mediated inhibition of tubulin polymerization causes inappropriate accumulation of G2/M regulators and leads to apoptosis.

Isochaihulactone-induced apoptosis in A549 cells after mitotic arrest. The mechanism by which apoptosis is induced by microtubule-damaging agents is not completely understood. The activation of aspartate-specific cysteine protease (caspase) represents a crucial step in the induction of drug-induced apoptosis, and cleavage of poly(ADP–ribose) polymerase (PARP) by caspase-3 is considered to be one of the hallmarks of apoptosis [36]. In our study, isochaihulactone was able to inhibit Bcl-2 expression, cause caspase-9 and caspase-3 cleavage, and PARP activation (Fig. 6A). Interesting, a time-course study showed that isochaihulactone-induced Bcl-2 phosphorylation, the cleavage of caspase-9 and PARP starting at the same point, suggesting that the isochaihulactone-induced Bcl-2 phosphorylation might be related apoptosis (Fig. 6B). Moreover, many microtubule-destabilizing agents are activators of caspase-9 that is involved in mitochondrial apoptosis [37,38]. Bcl-2 and Bcl-XL are known to inhibit apoptosis by regulating the mitochondrial membrane potential. Cytochrome *c* release needs for activation of caspase-9 and subsequent activation of caspase-3 [39]. Our data showed that increased phosphorylation of Bcl-2, activate caspase-9, and caspase-3 appeared to regulate the mitochondrial apoptotic pathway directly in the absence of active caspase-8.

Recent reports indicate that microtubule depolymerization agents, which arrest the cell cycle in G2/M phase, act through several types of kinases, leading to phosphorylation cascades and the activation of cyclin B1/cdc2 complex and Bcl-2 phosphorylation [40]. To investigate the molecular mechanism of isochaihulactone-induced G2/M arrest, the effect of various concentrations of kinase inhibitors was tested. Preliminary data show that the mitogen-activated protein kinase inhibitor PD98059 partially inhibited isochaihulactone-induced cdc2 phosphorylation and G2/M arrest (data not shown). This result suggests that isochaihulactone-induced G2/M arrest may involve the activation of some kinases, such as ERK1/2.

In clinical use, *Vinca* alkaloids including vincristine (Oncovin) and vinblastine (Velban) disrupt cellular division by binding to and inhibiting the polymerization of tubulin and are major drugs in treatment of Hodgkin's lymphoma and acute leukemia, respectively [41,42]. They have minimal effect

on carcinoma. Comparing with these drugs, our isochaihulactone showed against mainly carcinoma (non-small cell carcinoma of lung, ovary carcinoma, hepatoma, colon carcinoma, breast carcinoma, *etc.*) rather than sarcoma. Furthermore, vincristine can cause severe bone marrow suppression and neurotoxicity [43,44]. In contrast, isochaihulactone has no any significant abnormal findings on heart, liver, brain, bone marrow, kidney under histology examination (data not shown) and serology test even on high dosage (50 mg/kg).

In summary, isochaihulactone, a novel lignan compound isolated from BS-AE by bioassay-guided fractionation of active components, is a microtubule-depolymerizing agent that causes inappropriate expression of cyclin B1/cdc2 kinase, Bcl-2 phosphorylation, and finally initiates the apoptotic cascade. It is efficacious in suppressing various tumor cells growth and drug-resistant cells. Furthermore, it has considerable antitumoral efficacy *in vivo*. In the present study, isochaihulactone could be synthesize (method has not been published) and a series of this compound has been evaluated their biological activities for further drug development. These finding indicate isochaihulactone has high therapeutic potential and should be investigated further.

Acknowledgement

The work was supported by grant (Ref. No.: NSC94-2320-B303-001) from National Science Council, Taiwan, ROC.

REFERENCES

[1] Eisenberg DM, Davis RB, Ettner SL, Wilkey S, Van Rompay M, Kessler RC. Trends in alternative medicine use in the United States, 1990–1997: results of a follow-up national survey. J Am Med Assoc 1998;280:1569–75.
[2] Wang LG, Liu XM, Kreis W, Budman DR. The effects of antimicrotubule agents on signal transduction pathways of apoptosis: a review. Cancer Chemother Pharmacol 1999;44:355–61.
[3] Jordan A, Hadfield JA, Lawrence NJ, McGown AT. Tubules as a target for anticancer drugs: agents which interact with the mitotic spindle. Med Res Rev 1998;18:219–48.
[4] Kuo CC, Hsieh HP, Pan WY, Chen CP, Liou JP, Lee SJ, et al. BPR0L075, a novel synthetic indole compound with antimitotic activity in human cancer cells, exerts effective antitumoral activity in vivo. Cancer Res 2004;64:4621–8.
[5] Schwartsmann G, Ratain MJ, Cragg GM, Wang GE, Saijo N, Parkinson DR. Anticancer drug discovery and development throughout the world. J Clin Oncol 2002;20:47S–59S.
[6] Kelly K, Lovato LPJ, Livingston RB, Zangmeister J, Taylor SA, Roychowdhury D, et al. Southwest Oncology Group. Cisplatin, etoposide, and paclitaxel with granulocyte colony-stimulating factor in untreated patients with extensive-stage small cell lung cancer: a phase II trial of the Southwest Oncology Group. Clin Cancer Res 2001;7:2325–9.
[7] Zou Y, Fu H, Ghosh S, Farquhar D, Klostergaard J. Antitumor activity of hydrophilic paclitaxel copolymer prodrug using locoregional delivery in human orthotopic non-small cell lung cancer xenograft models. Clin Cancer Res 2004;10:7382–91.
[8] Kragelj B, Zaletel-Kragelj L, Sedmak B, Cufer T, Cervek J. Phase II study of radiochemotherapy with vinblastine in invasive bladder cancer. Radiother Oncol 2005;75:44–7.
[9] Kugler A, Haschemi R, Zoller G, Gross AJ, Kallerhoff M, Ringert RH. Anticancer drug discovery and development throughout the world. Urol Res 1997;25:240–50.
[10] Lu da Y, Huang M, Xu CH, Yang WY, Hu CX, Lin LP, et al. Anti-proliferative effects, cell cycle G2/M phase arrest and blocking of chromosome segregation by probimane and MST-16 in human tumor cell lines. BMC Pharmacol 2005;20:1–11.
[11] Schwartsmann G, Ratain MJ, Cragg GM. Anticancer drug discovery and development throughout the world. J Clin Oncol 2002;20:47S–59S.
[12] Jemal A, Thomas A, Murray T, Thun M. Cancer statistics, 2002. CA Cancer J Clin 2002;52:23–47.
[13] Cheng YL, Chang WL, Lee SC, Liu YG, Chen CJ, Lin SZ, et al. Acetone extract of *Angelica sinensis* inhibits proliferation of human cancer cells via inducing cell cycle arrest and apoptosis. Life Sci 2004;75:1579–94.
[14] Kao ST, Yeh CC, Hsieh CC, Yang MD, Lee MR, Liu HS. The Chinese medicine Bu-Zhong-Yi-Qi-Tang inhibited proliferation of hepatoma cell lines by inducing apoptosis via G0/G1 arrest. Life Sci 2001;69:1485–96.
[15] Vickers A. Botanical medicines for the treatment of cancer: rationale, overview of current data, and methodological considerations for phase I and II trials. Cancer Invest 2002;20:1069–79.
[16] Cheng YL, Chang WL, Lee SC, Liu YG, Lin HC, Chen CJ, et al. Acetone extract of *Bupleurum scorzonerifolium* inhibits proliferation of A549 human lung cancer cells via inducing apoptosis and suppressing telomerase activity. Life Sci 2003;73:2383–94.
[17] Cheng YL, Lee SC, Lin SC, Chang WL, Chen YL, Tsai NM, et al. Anti-proliferative activity of Bupleurum scrozonerifolium in A549 human lung cancer cells in vitro and in vivo. Cancer Lett 2005;222:183–93.
[18] Martello LA, Verdier-Pinard P, Shen HJ, He L, Torres K, Orr GA, et al. Elevated level of microtubule destabilizing factors in a taxol-resistant/dependent A549 cell line with α-tubulin mutation. Cancer Res 2003;63:448–54.
[19] Chang JY, Chang CY, Kuo CC, Chen LT, Wein YS, Kuo YH, et al. A novel microtubule inhibitor isolated from *Salvia miltiorrhizea* Bunge (Danshen) with antimitotic activity in multidrug-sensitive and resistant human tumor cells. Mol Pharmcol 2004;65:77–84.
[20] Hosono S, Lee CS, Chou MJ, Yang CS, Shih CH. Molecular analysis of the p53 alleles in primary hepatocellular carcinomas and cell lines. Oncogene 1999;6:237–43.
[21] Mickisch G, Fajta S, Keilhauer G, Schlick E, Tschada R, Alken P. Chemosensitivity testing of primary human renal cell carcinoma by a tetrazolium based microculture assay (MTT). Urol Res 1990;18:131–6.
[22] Bollag DM, McQueney PA, Zhu J. Epothilone, a new class of microtubule-stabilizing agents with a taxol-like mechanism of action. Cancer Res 1995;55:2325–33.
[23] Blagosklonny DM, Schulte TW, Nguyen P, Mimnaugh EG, Trepel J, Neckrs L. Taxol induction of p21/WAF1 and p53 requires c-raf-1. Cancer Res 1995;55:4623–6.
[24] van Engeland M, Ramaekers FC, Schutte B, Reutelingsperger CP. Annexin V-affinity assay: a review on an apoptosis detection system based on phosphatidylserine exposure. Cytometry 1998;31:1–9.
[25] Krajewski S, Tanaka S, Takayama S, Schibler MJ, Fenton W, Reed JC. Investigation of the subcellular distribution of the bcl-2 oncoprotein: residence in the nuclear, endoplasmic reticulum, and outer mitochondrial membranes. Cancer Res 1993;53:4701–14.

[26] Dumontet C, Sikic BI. Mechanisms of action of the resistance to antitubulin agents: microtubule dynamics, drug transport, and cell death. J Clin Oncol 1999;17:1061–70.
[27] Deng L, Tatebe S, Lin-Lee YC, Ishikawa T, Kuo MT. MDR and MRP gene families as cellular determinant factors for resistant to clinical anticancer agents. Cancer Treat Res 2002;112:49–66.
[28] Downing KH, Nogales E. Crystallographic structure of tubulin: Implication for dynamics and drug binding. Cell Struct Funct 1999;24:269–75.
[29] Bai R, Davidm DG, Pei XF, Ewelli JB, Nguyeni NY, Brossi A, et al. Mapping the binding site of colchicinoids on β-tubulin. J Biol Chem 2000;22:40443–52.
[30] Ravelli BG, Gigant B, Curmi PA, Jourdain I, Lachkar S, Sobel A, et al. Insight into tubulin regulation from a complex with colchicines and a stathmin-like domain. Nature 2004;11:428.
[31] Gigant B, Curmi PA, Jourdain I, Charbaut E, Lachkar S, Lebeau L, et al. The 4 Å X-ray structure of a tubulin:stathmin-like domain complex. Cell 2000;102: 809–16.
[32] Guillot C, Falette N, Paperin MP, Courtois S, Gentil-Perret A, Treilleux I, et al. $p21^{WAF1/CIP}$ response to genotoxic agents in wild type *TP53* expression breast primary tumors. Oncogene 1997;14:45–52.
[33] Bulavin DV, Higashimoto Y, Demidenko ZN, Meek S, Graves P, Phillips C, et al. Dual phosphorylation controls Cdc25 phosphatases and mitotic entry. Nat Cell Biol 2003;5:545–51.
[34] Gould KL, Nurse P. Tyrosine phosphorylation of the fission yeast $cdc2^{+}$ protein kinase regulates entry into mitosis. Nature 1989;342:39–45.
[35] Lammer C, Wagerer S, Saffrich R, Mertens D, Ansorge W, Hoffmann I. The cdc25B phosphatase is essential for the G2/M phase transition in human cells. J Cell Sci 1998;111:2445–53.
[36] Singh RP, Agrawal P, Yim D, Agarwal C, Agarwal R. Acacetin inhibits cell growth and cell cycle progression, and induces apoptosis in human prostate cancer cells: structure-activity relationship with linarin and linarin acetate. Carcinogenesis 2005;26:845–54.
[37] Susin SA, Lorenzo HK, Zamzami N. Mitochondrial release of caspase-2 and caspase-9 during the apoptosis process. J Exp Med 1999;189:381–94.
[38] Slee EA, Harte MT, Kluck RM, Wolf BB, Casiano CA, Newmeyer DD. Ordering the cytochrome c-initiated caspase cascade: hierarchical activation of caspases-2, -3, -6, -7, -8 and -10 in a caspase-9 dependent manner. J Cell Biol 1999;144:281–92.
[39] Du L, Lyle CS, Chambers TC. Characterisation of vinblastine induced BCL-XL and BCL-2 phosphorylation: evidence for a novel protein kinase and a coordinated phosphorylation/dephosphorylation cycle associated with apoptosis induction. Oncogene 2005;24:107–17.
[40] Liao CH, Pan SL, Guh JH, Chang YL, Pai HC, Lin CH, et al. Antitumor mechanism of evodiamine, a constituent from Chinese herb Edodiae fructus, in human multiple-drug resistant breast cancer NCI/ADR-RES cells in vitro and in vivo. Carcinogenesis 2005;26:968–75.
[41] Franklin J, Diehl V. Current clinical trails for the treatment of advanced-stage Hodgkin's disease: BEACOPP. Ann Oncol 2002;13:98–101.
[42] Kolb EA, Steinherz PG. A new multidrug reinduction protocol with topotecan, vinorelbine, thiotepa, dexamethasone, and gemcitabine for relapsed or refractory acute leukemia. Leukemia 2003;17:1962–72.
[43] Rebert CS, Pryor GT, Frick MS. Effects of vincristine, maytansine and *cis*-platinum on behavioral and electrophysiological indices of neurotoxicity in the rat. J Appl Toxicol 1984;4:330–8.
[44] Chae L, Moon HS, Kim SC. Overdose of vincristine: experience with a patient. J Korean Med Sci 1998;13:334–8.